Laboratori Nazionali di Frascati

Submitted to Nucl. Instr. & Meth. in Phys. Research.

LNF-89/036(P)
1 Giugno 1989

Revised Version
Giugno 1990

H. Bilokon, A. Castellina, B. D'Ettorre Piazzoli, G. Mannocchi, P. Picchi S. Vernetto:

UNDERGROUND SURVIVAL PROBABILITIES OF HIGH ENERGY MUONS IN THE DEPTH RANGE 3100-10100 hg/cm^2 OF STANDARD ROCK

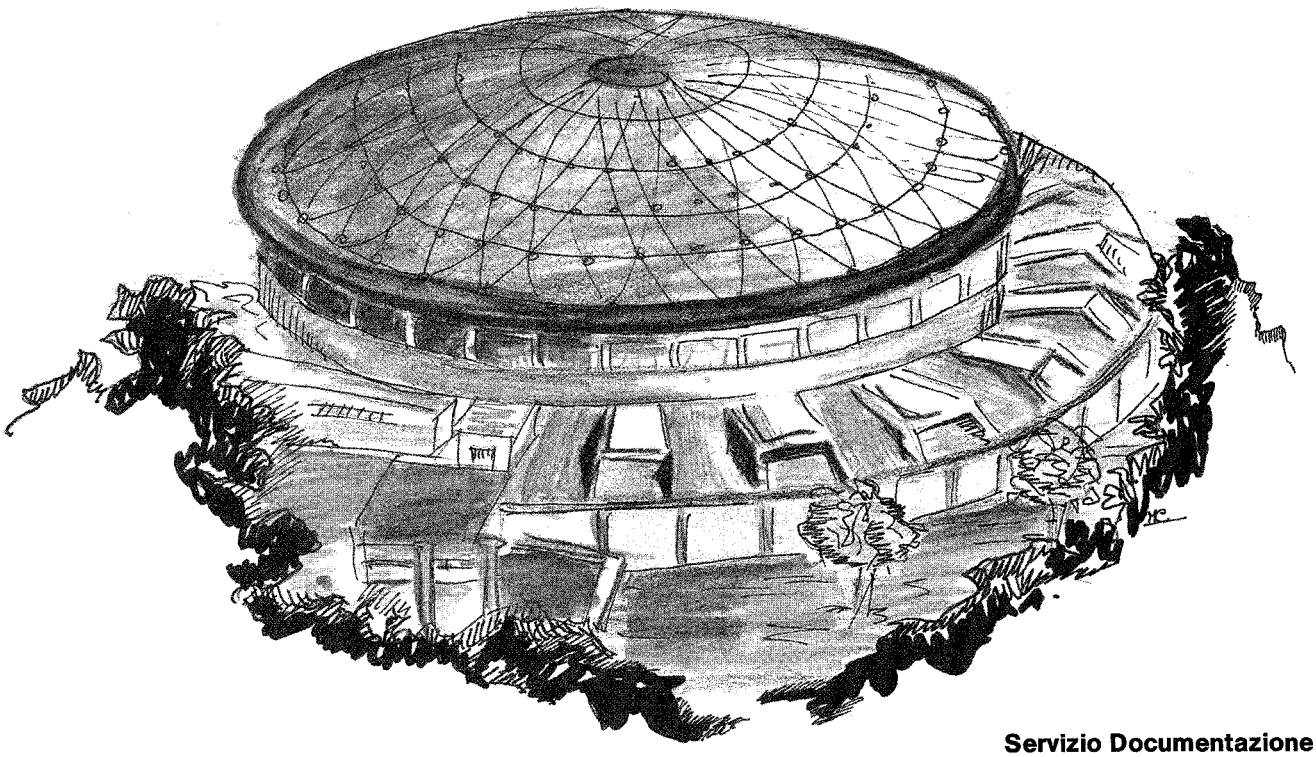

Servizio Documentazione
dei Laboratori Nazionali di Frascati
P.O. Box, 13 - 00044 Frascati (Italy)

INFN - Laboratori Nazionali di Frascati
Servizio Documentazione

LNF-89/036(P)
1 Giugno 1989

Revised Version
Giugno 1990

UNDERGROUND SURVIVAL PROBABILITIES OF HIGH ENERGY MUONS IN THE DEPTH RANGE 3100-10100 hg/cm^2 OF STANDARD ROCK

H. Bilokon[1)], A. Castellina[2)], B. D'Ettorre Piazzoli[1,2)], G. Mannocchi[1,2)], P. Picchi[1,3)] S. Vernetto[2)]

1) Laboratori Nazionali di Frascati dell'INFN - Frascati (Roma), Italy
2) Istituto di Cosmogeofisica del CNR - Torino, Italy
3) Istituto di Fisica Generale dell'Universita' - Torino, Italy

ABSTRACT

The propagation of high energy muons through thick layers of standard rock has been simulated by means of a Monte Carlo calculation. Muon survival probabilities have been calculated and tabulated for depths from 3100 down to 10100 hg/cm^2 in steps of 200 hg/cm^2. The influence of multiple scattering in rock has been found to be negligible. The uncertainty introduced by the ambiguity in describing the inelastic muon-nucleus interaction has been evaluated and found to be relatively small even for the maximum depth considered here.

1. - INTRODUCTION

Much effort has been devoted in cosmic ray physics to calculate the transport of muons through large thicknesses of rock with the purpose of correlating the depth-intensity measurements to the muon energy spectrum at sea level. The interest in such calculations has been renewed due to recent development of large underground detectors devoted to a search for the nucleon decay and astrophysical neutrinos.

The main problem is to account for electromagnetic processes other than ionization; in fact, at very high energies (> 100 GeV), bremsstrahlung, pair production and photonuclear interactions can contribute substantially to the muon energy loss. Moreover, bremsstrahlung and nuclear interactions lead to loss of a large fraction of energy in single rare events, thus

giving rise to large fluctuations. As a result, range straggling of ultrarelativistic muons becomes important and it is not possible to define a threshold energy for a muon reaching a given depth.

Dealing with the energy losses as discontinuous ones, the underground muon intensity $I_\mu(h)$ at a depth h is given by

$$I_\mu(h) = \int_{E_{min}}^{\infty} P(E,h)\, N(E) dE \qquad (1)$$

where P(E,h) is the survival probability for a muon of energy E at a depth h, N(E) is the differential energy spectrum of muons at the surface and E_{min} is the minimum energy for a muon to have any chance to survive up to a depth h. On the contrary, considering all energy losses as continuous, that is neglecting the straggling, the underground intensity is given by

$$\overline{I_\mu}(h) = \int_{E_0}^{\infty} N(E) dE$$

where E_0 is the energy corresponding to the range h. The quantities of interest are the survival probability P(E,h) or the correction factor $R(h) = I_\mu(h)/\overline{I_\mu}(h)$ which depends on the form of the muon spectrum.

The various methods of calculation which have been used are essentially of three types: numerical computations [1], analytical solutions [2] and Monte Carlo approach [3].

The last method allows one to take into account the energy dependence of cross sections and to avoid several approximations required by other techniques. On the other hand, a large number of particles has to be generated in order to achieve good statistical accuracy, since small values of the survival probabilities P(E,h) contribute strongly to the intensity, due to the sharply falling muon spectrum. The present generation of computers allows one to overcome this problem once some, although not critical, approximations are used in the sampling process. A limitation to this method is given by the fact that for each choice of cross section describing the physical process responsible for the muon energy loss, a new Monte Carlo procedure has to be started. In this respect, accurate enough expressions are provided for all processes, apart from the inelastic muon-nucleon cross section, which needs to be extrapolated up to few thenths TeV in calculating P(E,h) for large depths (> 7000 hg/cm^2).

An accurate one-dimensional Monte Carlo simulation of the passage of muons through large thicknesses of standard rock (Z=11, A=22) has been performed in order to obtain the survival probability P(E,h) as a function of the surface energy.

Calculations have been done for depths 3100 to 10100 hg/cm^2 in steps of 200 hg/cm^2. This interval covers the range of depths important for experiments at the Gran Sasso Laboratory. For each depth the energies corresponding to survival probabilities 1%, 3% .... up to 97% are tabulated. For any other value of E and h inside the quoted intervals the survival probability P(E, h) can be easily obtained with good accuracy by interpolation.

The most recent formulae for the cross section of the main processes contributing to the energy loss have been used. The theoretical description of the photonuclear interaction of high energy muons contains some ambiguity. The present calculations have been done for an energy dependent total photon-nucleus cross section.

The effects due to multiple Coulomb scattering as well as of using a constant photon-nucleus cross section have been evaluated and found negligible.

2. - FUNDAMENTAL PROCESSES

The energy loss dE/dx of muons may occur through:

a) processes with negligeable straggling (ionization and pair production), where the transferred energy E' is always a small fraction (of order m_e/m_μ) of the muon energy E. The cross section for these processes falls off so rapidly with È' ($1/v^2$ and $1/v^3$ respectively, v = E'/E) that they may be considered as giving continuous energy losses.

The mean energy loss (in MeV per g/cm^2) for ionization and excitation is given by [4]

$$\frac{dE}{dx} = 0.1535 \cdot \frac{1}{\beta_\mu^2}\left(\frac{Z}{A}\right)\cdot\left\{\ln\left(\frac{m_e E'_m}{I^2}\right) + .693 + 2\cdot\ln\frac{P_\mu}{m_\mu} + \frac{1}{4}\left(\frac{E'_m}{E}\right)^2 - 2\beta_\mu^2 - \delta - U\right\} \qquad (2)$$

where m_e is the electron mass, m_μ, β_μ and P_μ are the mass, velocity, and momentum of the muon; E'_m is the maximum energy the passing particle can transfer to an electron of the medium, given by

$$E'_m = 2m_e \cdot \frac{P_\mu{}^2}{m^2{}_e + m^2{}_\mu + 2\cdot m_e \cdot E}$$

Z, A, I are the average atomic number, atomic weight and ionization potential of the medium, δ is the density effect term and U is the shell correction term. The last term in eq.(2) is a very small quantity and can be neglected. For the density correction δ, we have used the parametrization given in [5]

$$\begin{aligned} \delta(X) &= 4.6052X + a(X_1 - X)^m + C \qquad && X_0 < X < X_1 \\ &= 4.6052X + C && X > X_1 \end{aligned}$$

where $X = \log_{10}(P_\mu/m_\mu)$. The values for Z, A, I, X_0, X_1, a, m, C relative to the standard rock are given by [6]

$$\begin{aligned} &Z = 11, \quad A = 22, \quad I = 148\ \text{eV} \\ &X_0 = 0.2, \quad X = 3.0 \\ &a = .14, \quad m = 3, \quad C = -3.99 \end{aligned}$$

At high energies (> 5 GeV) the useful parametrization

$$\frac{dE}{dx} = 1.88 + 0.077 \ln\left(E'_m/m_\mu\right)$$

can be used.

The mean energy loss for pair production, which dominates at high energies, has been calculated by integrating the differential cross section given by Kokulin and Petrukhin in [7], which includes the screening effect according to the Fermi-Thoms model

$$\frac{dE}{dx} = 2 \cdot E \frac{N}{A} \int_{v_{min}}^{v_{max}} v \cdot dv \int_0^{\rho_{max}} \left(\frac{d^2\sigma}{dv d\rho}\right) d\rho \qquad (3)$$

where

$$\frac{d^2\sigma}{dv d\rho} = \frac{2}{3\pi} \left(r_0 \cdot \alpha\right)^2 Z(Z+1) \frac{1-v}{v} \cdot \left[\Phi_e + \left(\frac{m_e}{m_\mu}\right)^2 \Phi_\mu\right]$$

N is the Avogadro number, α is the fine structure constant, r_0 is the classical electron radius and

$$v = \frac{\varepsilon^+ + \varepsilon^-}{E}, \quad \rho = \frac{\varepsilon^+ - \varepsilon^-}{\varepsilon^+ + \varepsilon^-}$$

are the fraction of energy lost and the asymmetry parameter of the electron-positron pair, (ε^+ and ε^- are the e^+ and e^- energies). The explicit expression for Φ_e and Φ_μ and for the integration limits are given in Appendix.

b) processes with straggling (bremsstrahlung and nuclear interactions), in which the particle may lose a large fraction of its energy in a single interaction because the cross section falls off rather slowly (~ 1/v) with increasing energy transfer. The relevant quantity for sampling purposes is the differential probability of a particle losing a fraction v of its energy per g/cm^2, given by

$$\frac{dP}{dv} = \frac{N}{A} \frac{d\sigma}{dv}$$

Bremsstrahlung provides the main contribution to the fluctuations in the muon energy loss. For it, a comprehensive treatment has been performed by Petrukhin and Shestakov [8], who give the following differential cross section

$$\frac{d\sigma}{dv} = 4 \cdot \alpha \cdot r_0^2 Z(Z+1) \left(\frac{m_e}{m_\mu}\right)^2 \frac{1}{v} \left[\frac{4}{3}(1-v) + v^2\right] \cdot \phi(\delta), \qquad v_{min} \le v \le v_{max} \qquad (4)$$

where v is the fraction of energy transferred to the photon and δ is the minimum momentum transfer to the nucleus. The explicit form of the function $\phi(\delta)$ and of the limits v_{min}, v_{max} is given in Appendix.

The inelastic muon-nucleus interaction contains many uncertainties. The description of this process involves a knowledge of the flux of virtual photons accompanying the muon and their interaction with the nuclear field. Because of the diffractive character of this interaction, (the average four-momentum transfer $<q^2>$ is about 0.1 $(GeV/c)^2$) the virtual photon behaviour is almost the same as that of real photons; however, the energy carried out by the virtual photon can increase to several TeV, whereas direct measurement of the γ-A cross section are available only up to about 200 GeV. Several models have been developed to describe this interaction in order to interpret the cosmic ray data. The differential cross section can be written in the following way.

$$\frac{d\sigma}{dv} = E \int_{q^2_{min}}^{q^2_{max}} \frac{d^2\sigma_{\mu A}}{dq^2\, dv} dq^2, \qquad v_{min} \le v \le v_{max} \tag{5}$$

with

$$\frac{d^2\sigma_{\mu A}}{dq^2\, dv} = A_{eff}(q^2, v) \frac{d^2\sigma_{\mu N}}{dq^2\, dv}$$

where q^2 is the modulus of the squared four momentum transferred to the nucleus, $v = \nu/E$ is the ratio of the energy transferred ν to the muon energy, A_{eff} the effective number of nucleon partecipating in the interaction of a photon in the nucleus, and $\sigma_{\mu N}$ is the inclusive cross-section for muon-nucleon scattering. Choices for A_{eff} and $\sigma_{\mu N}$ have been discussed in [9, 10]. We have used the results of Ref. [9] in which the virtual photon cross section is calculated within the framework of the generalized vector meson dominance (GVDM) model and the behaviour of the real photon cross section is assumed to increase with energy according to a $ln^2(\nu)$ dependence. The explicit form of $\sigma_{\mu N}$, A_{eff} and of the integration limits is given in Appendix.

Results from different assumptions are consistent at the 30% level. However, since the contribution of the muon photonuclear interaction to the energy loss is of the order of 10% of the total loss, the uncertainty is expected to be quite low up to very large depths.

The mean energy loss is related to the probability dP/dv as follows

$$\frac{dE}{dx} = E \int \frac{dP}{dv} \cdot v \cdot dv = E \cdot b(E) \,, \tag{6}$$

so that the total average energy loss is usually written as

$$\left(\frac{dE}{dx}\right)_{total} = a_{ion}(E) + E \cdot [b_{pp}(E) + b_b(E) + b_n(E)]$$

where the first term represents the contribution from ionization and $b_{pp}(E)$ is defined through the eq. (3).

The energy loss coefficients $b_i(E_\mu)$ for pair production (pp) bremmstrahlung (b) and nuclear interaction (n) are easily calculated as

$$b_i(E) = \frac{N}{A}\int \frac{d\sigma}{dv}\, v \cdot d \cdot v \left[\frac{g}{cm^2}\right]^{-1}$$

The contribution of each process to the totale energy loss is shown in Fig. 1. The ionization term is dominant up to about 200 GeV and from then on becomes less and less important.

3. - MUON PROPAGATION IN ROCK

A Monte Carlo technique has been adopted to simulate the propagation of high energy muons in rock. The muon is transported underground by dividing the total depth h in steps Δt and calculating the energy loss in each element for both the continuous and the stochastic processes. The stochastic energy loss in sampled through the function

$$P(\Delta t ; >v) = \Delta t \int_v^{v_{max}} \frac{dP}{dv}\, dv \qquad v_{min} < v_{cut} \leq v \leq v_{max}$$

which is the probability of a particle losing more than a fraction v of its energy in a slab of thickness Δt. The cut-off value v_{cut} is defined such that the energy losses in collisions with energy transfer $< v_{cut} \cdot E$ are accounted for on the average as the continuous ones. Energy losses $> v_{cut} \cdot E$ are found by generating a random number to correspond to the probability $P(\Delta t; > v)$. The step Δt size and v_{cut} have been chosen such that $P(\Delta t; > v) = 0.1$ in order to make the probability of two or more collisions in the same depth unit quite unlikely. In practice, we have assumed $\Delta t \leq 25$ hg/cm^2. This condition defines a very small cut off value v_{cut} corresponding to a vanishing continuous energy loss in the slab. This choice increase considerably the computing time but avoid any systematical bias in the estimate of the fluctuations.

The stochastic energy loss $v \cdot E$ is added to the continuous energy losses calculated from eqs.(2) and (3) to obtain the total energy loss in Δt. Then the energy of the muon is reduced by this quantity and the process repeated for the next element.

We have defined a limit energy of 5 GeV above which all processes are included. At lower energies, only ionization loss is taken into account, the contribution of the other

processes being more than 3 orders of magnitude smaller. When the muon energy falls below 5 GeV the range-energy relationship, calculated integrating eq.(2), is used to obtain the residual energy of surviving muons. Surviving muons are defined as those having residual total energy greater than .5 GeV. As a result, this simulation allows us to evaluate both the survival probability and the local energy spectrum (calculations of the local energy distribution have already been published, [11]. Experimental results [12] are in excellent agreement with these predictions).

4. - RESULTS

Calculations have been carried out for 36 different depths from 3100 down to 10100 hg/cm^2 in step of 200 hg/cm^2. The results are presented in Table I which provides the logarithm of the muon energy y(E) = ln E (GeV) corresponding to survival probabilities running from 1% to 97% in steps of 2%.

An accurate representation of P(E, h) outside this interval is not relevant because, due to the shape of the cosmic muon spectrum rapidly falling with energy as $E^{-\gamma}$, $\gamma = 2 \div 4$, the biggest contribution to the underground intensities comes from energies where the survival probability is in the region 10% - 60%.

The values of y(E) listed in Table I have been obtained according to the following procedure. Firstly, the survival probability is calculated at each depth for at least 50 arguments lying in the interval $y(E_{min}) \div y(E_{max})$, where E_{min} and E_{max} are the energies corresponding to survival probabilities of ~ .5% and ~ 98% respectively. For each energy a very large number N of muons has been traced in order to obtain a relative precision $\sigma_p/P = \sqrt{(1-P)/(N \cdot P)} \sim 5\%$. However the number of transported muons of initial energy corresponding to survival probabilities of about 5%, 25%, 45%, 65%, 85% was enough to get a precision ~ 1.5%.

Then cubic spline curves have been used to fit smooth functions to the calculated points. The resulting continuous curves, shown in Fig. 2, provide the tabulated values of y(E). The fractional statistical uncertainty is estimated less han 5% on average.

The departure of the survival probability from a step-like function is a consequence of the fluctuations in energy loss. The effect of straggling is relevant, as shown in Fig. 3 where the range distributions for muons of energies E = 1, 10, 50 TeV are plotted. The shape of the range distribution is asymmetric, with a long tail for short ranges. The average is therefore different from the most probable range.

As an illustration, these results have been applied to the calculation of underground intensities using the expression (1) and taking the muon energy differential spectrum in the form $N(E)dE = K \cdot E^{-\gamma} dE$ with K = 19.17 and $\gamma = 3.71$ [13]. In performing the integration, the probability P(E, h) has been evaluated for each specific argument E by interpolation. The resulting variation of the muon intensity with depth underground for the range 3100 to 10100

hg/cm^2 s.r. is shown in Fig. 4. We note that also in the simplified case of a muon spectrum following a power law with constant slope the shape of the muon intensity underground cannot be represented by an unique exponential law since the steepness is decreasing with increasing depth.

The previous results have been obtained by means of a one-dimensional model for muon transport in which the multiple Coulomb scattering is neglected. This process causes the effective thickness of the absorber to be greater than the actual geometrical path. A three-dimensional transport, accounting for multiple Coulomb scattering, has been developed in order to determine the angular and lateral spread of muons at high depths[14]. Such information is very important for multiple muon physics and muon astronomy with underground detectors. The lengthning of the path is effective only at very low energies, and is practically concentrated at the end of the range, so that its influence on the survival probabilities at the depths considered here is irrelevat. In the least favourable case, h=3100 hg/cm^2 and muon energy near threshold [P(E,h) < 10%], a relative difference of a few percent has been found.

The effect of using a different extrapolation at high energies of the photon-nucleon cross section has been investigated. Survival probabilities obtained assuming a constant cross section $\sigma_{\gamma N}(\nu)$ = 125 μb have been calculated.A difference is found at depths greater than 6000 hg/cm^2. In Fig. 5 the survival probabilities at three different depths calculated according to the two different assumption are compared. At low energies the curves overlap, at high energies they tend asymptotically to the same value. A maximum difference of about 5% has been found at 10100 hg/cm^2. Accordingly, sea level muon energy spectrum and underground intensities should be known with a comparable accuracy in order that meaningful information on the photonuclear cross section at high energies could be inferred.

CONCLUSIONS

Survival probabilities of muons in the depth range 3100-10100 hg/cm^2 of standard rock have been calculated by a Monte Carlo method using a detailed description of the processes contributing to the energy loss of muons in matter. Results have been fitted to continuous curves and then tabulated to provided data useful for numerical applications in interpreting underground measurements. These include, for instance, the derivation of the atmospheric muon energy spectrum [13], and the calculation of the angular enhancement functions for underground muons used in deriving the prompt muon contribution to the atmospheric muon intensity [15].

A comparison made with results from a three-dimensional version of the same Monte Carlo shows that the present one-dimensional model for muon transport is well adequate to calculate the survival probability at depths greater than 3000 hg/cm^2 of standard rock.

APPENDIX - Cross Section Formulae

i) Direct pair production

The terms Φ_e and Φ_μ in eq.(3) include first and second order processes and also contain corrections arising from atomic and nuclear form factors. Their explicit form, as given in [7], is

$$\Phi_\mu = \left\{ \left[(1+\rho^2)\left(1+\frac{3}{2}\beta\right) - (1/\xi)\,(1+2\beta)(1-\rho^2) \right] \cdot \log(1+\xi) + \frac{\xi(1-\rho^2-\beta)}{1+\xi} + (1+2\beta)(1-\rho^2) \right\} L_\mu$$

$$\Phi_e = \left\{ \left[(2+\rho^2)(1+\beta) + \xi(3+\rho^2) \right] \log(1+1/\xi) + \frac{1-\rho^2-\beta}{1+\xi} - (3+\rho^2) \right\} L_e$$

where

$$\xi = \left(\frac{m_\mu \cdot v}{2m_e}\right)^2 \left(\frac{1-\rho^2}{1-v}\right)$$

$$\beta = \frac{v^2}{2(1-v)}$$

ρ, v have the same meaning as given in the text.

The functions L_e and L_μ are given by

$$L_e = \ln \frac{RZ^{-1/3}\sqrt{(1+\xi)(1+Y_e)}}{1+\dfrac{2m_e\sqrt{e}\,RZ^{-1/3}(1+\xi)(1+Y_e)}{Ev(1-\rho^2)}} - \frac{1}{2}\ln\left[1+\left(\frac{3}{2}\frac{m_e}{m_\mu}Z^{1/3}\right)^2 \cdot (1+\xi)(1+Y_e)\right]$$

$$L_\mu = \ln \frac{(2/3)\,(m_\mu/m_e)\,RZ^{-2/3}}{1+\dfrac{2m_e\sqrt{e}\,RZ^{-1/3}(1+\xi)(1+Y_\mu)}{Ev(1-\rho^2)}} -$$

where R = 189 is the value of the radiation logarithm and e = 2.718

$$Y_e = \frac{5-\rho^2+4\beta\,(1+\rho^2)}{2(1+3\beta)\ln(3+1/\xi)-\rho^2-2\beta(2-\rho^2)}$$

$$Y_e = \frac{4 - \rho^2 + 3\beta\,(1+\rho^2)}{(1+\rho^2)\left(\frac{2}{3}+2\beta\right)\ln(3+\xi)+1-(3/2)\rho^2}$$

The integration limits are

$$\frac{4m_e}{E} \le v \le 1 - \frac{3\sqrt{e}\cdot m_\mu}{4E} Z^{1/3}$$

$$0 \le |p| \le \left(1 - \frac{6m_\mu^2}{E^2(1-v)}\sqrt{1-\frac{4m_e}{Ev}}\right)$$

ii) Bremsstrahlung

The function $\phi(\delta)$ in eq.(4)is given by [8]

$$\Phi(\delta) = \ln \frac{\frac{2}{3} R \frac{m_\mu}{m_e} Z^{-2/3}}{1 + \frac{R\cdot\sqrt{e}}{m_e}\cdot\delta\cdot Z^{-2/3}}$$

where $\delta = \dfrac{m_\mu^2 \cdot v}{2E(1-v)}$ is the minimum momentum transfer to the nucleus, R and e have the same meaning as defined in i). This expression takes into account the correction from the nucleon form factor and is valid for $Z \ge 10$. The integration limits are

$$v_{min} = 0$$

$$v_{max} = 1 - \frac{3}{4}\sqrt{e}\cdot\frac{m_\mu}{E}\cdot Z^{1/3}$$

iii) Nuclear interaction

In the one-photon-exchange approximation the cross section of inelastic muon-nucleon scattering is written as

$$\frac{d\sigma^2_{\mu N}}{dq^2 d\nu} = \frac{4\pi\alpha^2}{q^4}\,\frac{1}{E^2 - m_\mu^2}\cdot\frac{1}{\nu}\cdot\left[E(E-\nu) - \frac{1}{4}q^2 + \left(\frac{1}{2} - \frac{m_\mu^2}{q^2}\right)\frac{q^2+\nu^2}{1+R(\nu,q^2)}\right]\nu\cdot W_2(q^2,\nu)$$

Within the framework of GVMD the structure function $\nu W^2(\nu,q^2)$ is given by [16]

$$\nu W^2(\nu,q^2) = \frac{\nu K}{4\pi^2\alpha}\,\frac{q^2}{q^2+\nu^2}\,\sigma_t(\nu, q^2)\,(1+R)$$

where $K = \nu - q^2/2M$, with M = nucleon mass, $\sigma_t(\nu, q^2)$ is the transverse virtual photo-absorption cross section and $R = \sigma_s/\sigma_t$ is the ratio of the cross sections of the longitudinal and transverse polarised virtual photons. In this approach σ_t is related to the real photon cross section as follows

$$\sigma_t(\nu, q^2) = \sigma_{\gamma N}(\nu)\,\frac{1}{1+q^2/\overline{m}^2} \quad \text{with } \overline{m}^2 = 0.36\ (\text{GeV})^2$$

Different assumptions about R lead to a negligible effect in the cross section [10]. The expression $R = q^2/\nu^2$, resulting from the scaling law in the naive parton model, has been used. The total photoproduction cross section has been calculated in Ref. [17] according to GVDM and is well represented by the formula

$$\sigma_{\gamma N}(\nu) = 114.3 + 1.647\,\ln^2(0.0213\,\nu)\ \mu b \qquad 10\ \text{GeV} < \nu < 10^6\ \text{GeV}$$

The shadowing effect, resulting in a smaller than linear A dependence ($A_{eff}/A < 1$), has been taken into account using the parametrization of Ref. [9] derived assuming that the virtual photons behave partly as vector-meson-like and partly point-like

$$A_{eff}\,(\nu, q^2) = A\left[.22 + .78\cdot\Delta\,(\nu, q^2)\cdot\frac{1}{1+q^2/\overline{m}^2}\right]$$

$$\text{with } \Delta(\nu, q^2) = \begin{cases} A^{-0.11} & \text{for } q^2 \le 0.25\ (\text{GeV})^2 \\ 1 & \text{for } q^2 > 0.25\ (\text{GeV})^2 \end{cases}$$

No difference has been assumed for protons and neutrons in the nucleus.

The kinematics limits in eq. (5) are given by

$$\nu_{min} = \nu_{min}/E$$

$$\nu_{max} = \nu_{max}/E$$

with

$$\nu_{min} = m_\pi + (m^2{}_\pi/2M)$$

$$\nu_{max} = E - \frac{M}{2}\left(1 + \frac{m_\mu^2}{M^2}\right)$$

and

$$q^2{}_{min} = \frac{m_\mu^2\,\nu^2}{E(E-\nu)} - \frac{m_\mu^4}{2E(E-\nu)}$$

$$q^2{}_{max} = 2M\,(\nu - m_\pi) - m^2{}_\pi$$

where m_π and M are the masses of the pion and nucleon respectively.

REFERENCES

1) S. Miyake, V.S. Narasimham and P.V. Ramana Murthy; Nuovo Cimento 32, 1524 (1964); H. Oda and T. Murayama; J. Phys. Soc. Japan 20, 1549 (1965); B.S. Meyer, J.P.F. Sellschop, M.F. Crouch, W.R. Kropp, H.W. Sobel, H.S. Gurr, J. Lathrop and F. Reines D1, 2229 (1970).
2) K. Kobayakawa, Nuovo Cimento B47, 156 (1967); E. Kiraly, P. Kirady and J.L. Osborne, J. Phys. A: Gen. Phys. 5, 444 (1972); V.I. Gurentsov, G.T. Zatsepin and E.D. Mikhal'chi Sov. J. Nucl. Phys. 23, 527 (1976).
3) J.L. Osborne, A.W. Wolfendale and E.C.M. Young, J. Phys. A: Gen.Phys. 1, 55 (1968); L. Bergamasco and P. Picchi, Nuovo Cimento B3, 134 (1970).
4) R.M. Sternheimer, Phys. Rev. 88, 851 (1952).
5) R.M. Sternheimer and R.F. Peierls, Phys. Rev. B3, 3681 (1971).
6) B.C. Rastin, J. Phys. G: Nucl. Phys. 10, 1609 (1984).
7) R.P. Kokoulin and A.A. Petrukhin, Proc. 12th Int. Conf. on Cosmic Rays, Hobart, 6, 2436 (1971).
8) A.A. Petrukhin and V.V. Shestakov, Can. J. Phys. 46S, 377 (1968).
9) Y. Minorikawa, T. Kitamura and K. Kobayakawa, Nuovo Cimento C4, 471 (1981) .
10) W.D. Dau, W. Constandt and H. Jokisch, J. Phys. G: Nucl. Phys. 9, 391 (1983).
11) A. Castellina, B. D'Ettorre Piazzoli, G. Mannocchi, P. Picchi, S. Vernetto, H. Bilokon and E. Meroni, Lett. Nuovo Cimento 44, 401 (1985).
12) M. Calicchio, C. De Marzo, O. Erriquez, C. Favuzzi, N. Giglietto, E. Nappi, F. Posa and P. Spinelli, Phys. Lett. B193, 131 (1987).
13) L. Bergamasco, A. Castellina, B. D'Ettorre Piazzoli, G. Mannocchi, P. Picchi, S. Vernetto and H. Bilokon, Nuovo Cimento C6, 569 (1983).
14) H. Bilokon, A. Castellina, B. D'Ettorre Piazzoli, A. Campos Fauth, G. Mannocchi, E. Meroni, P. Picchi and S. Vernetto, Proc. 20th ICRC, Moscow, 9, 199 (1987).
15) A. Castellina, B. D'Ettorre Piazzoli, G. Mannocchi, P. Picchi, S. Vernetto and H. Bilokon, Nuovo Cimento C8, 93 (1985).
16) R. Devenish and D. Schildknecht, Phys. Rev. D14, 93 (1976).
17) L.B. Bezrukov and E.V. Bugaev, Sov. J. Nucl. Phys. 32, 847 (1980).

TABLE I - The logarithmic muon energy y(E) = ln E(GeV) corresponding to survival probabilities 1%, 3%, ...97%, tabulated for depths from 3100 to 10100 hg/cm^2 of standard rock.

P(E,h)	3100	3300	3500	3700	3900	4100	4300
1	6.975	7.065	7.148	7.239	7.312	7.389	7.471
3	6.978	7.069	7.153	7.243	7.319	7.399	7.481
5	6.982	7.072	7.158	7.248	7.326	7.410	7.491
7	6.985	7.077	7.164	7.253	7.334	7.421	7.503
9	6.989	7.081	7.170	7.258	7.343	7.431	7.515
11	6.993	7.086	7.176	7.264	7.352	7.440	7.528
13	6.997	7.091	7.183	7.272	7.362	7.452	7.541
15	7.003	7.097	7.191	7.280	7.373	7.465	7.556
17	7.008	7.104	7.200	7.289	7.385	7.478	7.572
19	7.014	7.112	7.210	7.300	7.398	7.494	7.589
21	7.021	7.120	7.220	7.313	7.413	7.510	7.608
23	7.029	7.130	7.232	7.327	7.426	7.527	7.627
25	7.037	7.141	7.245	7.344	7.442	7.545	7.648
27	7.047	7.153	7.259	7.362	7.460	7.565	7.671
29	7.059	7.167	7.275	7.381	7.483	7.589	7.696
31	7.071	7.182	7.291	7.401	7.505	7.613	7.721
33	7.086	7.199	7.309	7.421	7.530	7.639	7.749
35	7.101	7.217	7.328	7.441	7.553	7.665	7.778
37	7.118	7.236	7.349	7.462	7.579	7.693	7.808
39	7.135	7.256	7.370	7.483	7.607	7.723	7.840
41	7.154	7.277	7.393	7.506	7.637	7.755	7.873
43	7.175	7.299	7.418	7.530	7.669	7.787	7.905
45	7.200	7.323	7.445	7.557	7.699	7.820	7.941
47	7.221	7.348	7.473	7.586	7.729	7.854	7.978
49	7.251	7.375	7.503	7.618	7.762	7.889	8.017
51	7.281	7.405	7.535	7.654	7.798	7.929	8.059
53	7.311	7.437	7.569	7.693	7.839	7.973	8.106
55	7.347	7.473	7.605	7.735	7.880	8.016	8.153
57	7.379	7.512	7.645	7.780	7.922	8.062	8.201
59	7.414	7.553	7.688	7.827	7.969	8.110	8.252
61	7.458	7.596	7.736	7.878	8.022	8.166	8.310
63	7.504	7.639	7.790	7.932	8.079	8.225	8.372
65	7.551	7.689	7.849	7.994	8.143	8.292	8.441
67	7.600	7.747	7.908	8.059	8.210	8.362	8.514
69	7.660	7.809	7.975	8.130	8.284	8.437	8.591
71	7.720	7.878	8.049	8.210	8.367	8.523	8.679
73	7.793	7.950	8.130	8.296	8.455	8.614	8.774
75	7.877	8.040	8.220	8.394	8.555	8.717	8.879
77	7.956	8.133	8.312	8.499	8.663	8.828	8.993
79	8.070	8.241	8.415	8.613	8.781	8.949	9.117
81	8.171	8.360	8.539	8.738	8.909	9.080	9.252
83	8.308	8.497	8.681	8.890	9.064	9.237	9.411
85	8.449	8.640	8.841	9.050	9.227	9.404	9.581
87	8.617	8.823	9.038	9.232	9.415	9.599	9.789
89	8.820	9.039	9.251	9.462	9.649	9.836	10.023
91	9.082	9.309	9.530	9.746	9.936	10.127	10.317
93	9.401	9.633	9.846	10.079	10.280	10.481	10.682
95	9.822	10.083	10.335	10.546	10.757	10.967	11.178
97	10.531	10.781	11.032	11.287	11.527	11.727	11.967

Table I Continued

P(E,h)	4500	4700	4900	5100	5300	5500	5700
1	7.542	7.615	7.687	7.755	7.824	7.893	7.961
3	7.554	7.623	7.703	7.774	7.846	7.918	7.989
5	7.565	7.640	7.720	7.794	7.868	7.943	8.017
7	7.579	7.657	7.737	7.814	7.891	7.968	8.045
9	7.595	7.675	7.755	7.835	7.915	7.995	8.075
11	7.610	7.692	7.774	7.857	7.939	8.022	8.105
13	7.626	7.710	7.794	7.879	7.965	8.050	8.136
15	7.642	7.728	7.814	7.903	7.991	8.079	8.167
17	7.660	7.748	7.836	7.927	8.018	8.109	8.200
19	7.679	7.769	7.859	7.953	8.047	8.140	8.234
21	7.700	7.792	7.884	7.975	8.071	8.167	8.264
23	7.721	7.815	7.909	8.004	8.103	8.201	8.300
25	7.744	7.840	7.936	8.035	8.135	8.236	8.336
27	7.769	7.867	7.965	8.067	8.169	8.271	8.373
29	7.795	7.895	7.995	8.101	8.204	8.307	8.410
31	7.823	7.925	8.027	8.136	8.241	8.346	8.451
33	7.853	7.957	8.061	8.172	8.279	8.386	8.493
35	7.884	7.990	8.096	8.210	8.312	8.422	8.537
37	7.917	8.025	8.134	8.250	8.354	8.466	8.584
39	7.949	8.063	8.173	8.292	8.396	8.512	8.633
41	7.984	8.103	8.215	8.335	8.444	8.561	8.683
43	8.023	8.141	8.258	8.379	8.494	8.611	8.735
45	8.062	8.183	8.304	8.425	8.544	8.663	8.790
47	8.102	8.227	8.351	8.474	8.597	8.719	8.845
49	8.145	8.273	8.400	8.524	8.650	8.776	8.903
51	8.190	8.321	8.452	8.577	8.706	8.835	8.964
53	8.239	8.372	8.506	8.632	8.765	8.897	9.028
55	8.289	8.425	8.561	8.690	8.826	8.962	9.094
57	8.341	8.481	8.620	8.751	8.890	9.029	9.164
59	8.393	8.534	8.676	8.817	8.958	9.100	9.237
61	8.454	8.598	8.742	8.886	9.030	9.174	9.315
63	8.519	8.665	8.812	8.959	9.106	9.252	9.397
65	8.590	8.739	8.888	9.037	9.186	9.335	9.486
67	8.665	8.817	8.968	9.120	9.272	9.423	9.580
69	8.744	8.898	9.052	9.205	9.363	9.518	9.680
71	8.836	8.992	9.149	9.305	9.462	9.620	9.789
73	8.933	9.092	9.251	9.411	9.570	9.729	9.899
75	9.041	9.202	9.364	9.526	9.688	9.849	10.022
77	9.157	9.322	9.486	9.651	9.816	9.980	10.154
79	9.285	9.452	9.620	9.788	9.955	10.123	10.290
81	9.423	9.594	9.766	9.937	10.108	10.280	10.441
83	9.584	9.758	9.932	10.105	10.278	10.452	10.631
85	9.758	9.935	10.113	10.290	10.467	10.644	10.834
87	9.966	10.149	10.332	10.516	10.699	10.882	11.065
89	10.210	10.397	10.584	10.771	10.958	11.144	11.325
91	10.507	10.698	10.888	11.078	11.269	11.459	11.663
93	10.882	11.083	11.284	11.485	11.686	11.887	12.080
95	11.389	11.600	11.811	12.021	12.232	12.443	12.643
97	12.202	12.437	12.678	12.907	13.138	13.359	13.569

Table I Continued

P(E,h)	5900	6100	6300	6500	6700	6900	7100
1	8.030	8.099	8.167	8.236	8.304	8.373	8.441
3	8.061	8.132	8.204	8.276	8.347	8.419	8.490
5	8.092	8.166	8.240	8.315	8.389	8.463	8.538
7	8.123	8.200	8.277	8.354	8.431	8.508	8.585
9	8.155	8.236	8.316	8.396	8.476	8.556	8.636
11	8.188	8.270	8.353	8.436	8.518	8.601	8.684
13	8.221	8.307	8.392	8.478	8.563	8.649	8.734
15	8.255	8.343	8.431	8.520	8.608	8.696	8.784
17	8.291	8.382	8.472	8.563	8.654	8.745	8.836
19	8.328	8.421	8.515	8.609	8.702	8.796	8.890
21	8.360	8.456	8.552	8.648	8.745	8.841	8.937
23	8.398	8.497	8.595	8.693	8.792	8.890	8.989
25	8.437	8.537	8.637	8.738	8.838	8.939	9.039
27	8.475	8.578	8.680	8.782	8.884	8.986	9.088
29	8.513	8.616	8.720	8.823	8.929	9.034	9.140
31	8.556	8.661	8.766	8.871	8.978	9.085	9.192
33	8.600	8.707	8.814	8.920	9.029	9.138	9.247
35	8.641	8.751	8.862	8.972	9.082	9.192	9.303
37	8.691	8.802	8.913	9.025	9.137	9.248	9.360
39	8.743	8.854	8.967	9.080	9.193	9.305	9.418
41	8.795	8.908	9.022	9.136	9.250	9.363	9.477
43	8.850	8.965	9.080	9.196	9.311	9.426	9.541
45	8.907	9.025	9.141	9.257	9.373	9.490	9.606
47	8.965	9.086	9.204	9.321	9.438	9.555	9.672
49	9.027	9.151	9.269	9.388	9.507	9.626	9.745
51	9.091	9.218	9.338	9.458	9.579	9.700	9.820
53	9.158	9.288	9.410	9.532	9.655	9.777	9.899
55	9.227	9.361	9.485	9.609	9.733	9.858	9.982
57	9.301	9.436	9.563	9.688	9.814	9.940	10.066
59	9.376	9.515	9.644	9.772	9.901	10.029	10.158
61	9.456	9.597	9.729	9.860	9.991	10.122	10.253
63	9.540	9.683	9.816	9.949	10.082	10.214	10.347
65	9.629	9.774	9.910	10.045	10.181	10.316	10.452
67	9.725	9.870	10.008	10.146	10.284	10.422	10.561
69	9.826	9.972	10.113	10.254	10.395	10.536	10.678
71	9.935	10.081	10.225	10.370	10.514	10.658	10.802
73	10.050	10.198	10.347	10.495	10.644	10.792	10.941
75	10.176	10.328	10.480	10.631	10.783	10.935	11.087
77	10.314	10.470	10.625	10.780	10.936	11.091	11.246
79	10.456	10.616	10.776	10.937	11.097	11.258	11.418
81	10.607	10.773	10.939	11.105	11.271	11.437	11.602
83	10.798	10.966	11.134	11.302	11.470	11.638	11.806
85	11.003	11.173	11.343	11.514	11.684	11.854	12.024
87	11.237	11.410	11.582	11.755	11.928	12.101	12.274
89	11.516	11.692	11.867	12.043	12.219	12.394	12.570
91	11.864	12.043	12.222	12.401	12.580	12.759	12.937
93	12.273	12.460	12.646	12.833	13.020	13.207	13.393
95	12.844	13.044	13.244	13.443	13.643	13.843	14.042
97	13.781	13.998	14.207	14.416	14.632	14.853	15.072

Table I Continued

P(E,h)	7300	7500	7700	7900	8100	8300	8500
1	8.510	8.579	8.647	8.716	8.785	8.853	8.922
3	8.562	8.634	8.705	8.777	8.848	8.920	8.991
5	8.612	8.686	8.761	8.835	8.909	8.984	9.058
7	8.663	8.740	8.817	8.894	8.971	9.048	9.126
9	8.716	8.796	8.876	8.956	9.036	9.116	9.196
11	8.767	8.850	8.932	9.015	9.097	9.180	9.263
13	8.820	8.905	8.991	9.076	9.162	9.247	9.333
15	8.872	8.960	9.048	9.137	9.225	9.313	9.401
17	8.927	9.018	9.108	9.199	9.290	9.381	9.472
19	8.983	9.077	9.170	9.264	9.358	9.451	9.545
21	9.033	9.129	9.225	9.321	9.417	9.514	9.610
23	9.087	9.186	9.285	9.383	9.482	9.581	9.680
25	9.140	9.240	9.342	9.443	9.545	9.646	9.748
27	9.190	9.292	9.397	9.502	9.607	9.711	9.816
29	9.246	9.352	9.458	9.564	9.671	9.777	9.883
31	9.300	9.407	9.516	9.625	9.733	9.842	9.951
33	9.356	9.464	9.576	9.687	9.799	9.910	10.021
35	9.413	9.523	9.637	9.752	9.866	9.980	10.095
37	9.472	9.583	9.700	9.817	9.934	10.051	10.167
39	9.531	9.644	9.763	9.883	10.002	10.122	10.241
41	9.591	9.705	9.827	9.950	10.072	10.194	10.316
43	9.656	9.771	9.896	10.020	10.145	10.270	10.394
45	9.722	9.839	9.965	10.092	10.219	10.345	10.472
47	9.790	9.907	10.035	10.164	10.293	10.421	10.550
49	9.864	9.983	10.113	10.243	10.372	10.502	10.631
51	9.940	10.061	10.192	10.324	10.455	10.587	10.715
53	10.021	10.144	10.276	10.408	10.540	10.672	10.805
55	10.106	10.231	10.364	10.498	10.632	10.765	10.899
57	10.192	10.318	10.454	10.590	10.726	10.862	10.997
59	10.286	10.415	10.552	10.690	10.827	10.964	11.101
61	10.384	10.516	10.655	10.793	10.932	11.071	11.210
63	10.480	10.612	10.755	10.898	11.040	11.183	11.326
65	10.588	10.723	10.864	11.013	11.155	11.303	11.448
67	10.699	10.837	10.980	11.125	11.274	11.425	11.575
69	10.819	10.960	11.101	11.248	11.401	11.561	11.712
71	10.947	11.091	11.235	11.381	11.537	11.707	11.857
73	11.090	11.238	11.383	11.535	11.685	11.851	12.010
75	11.238	11.390	11.539	11.701	11.846	12.012	12.175
77	11.402	11.557	11.711	11.877	12.020	12.189	12.349
79	11.578	11.739	11.900	12.051	12.213	12.382	12.535
81	11.769	11.934	12.095	12.255	12.416	12.576	12.736
83	11.974	12.142	12.305	12.469	12.632	12.796	12.960
85	12.195	12.365	12.533	12.700	12.868	13.035	13.203
87	12.446	12.619	12.790	12.961	13.132	13.303	13.474
89	12.745	12.921	13.094	13.267	13.441	13.614	13.787
91	13.116	13.295	13.473	13.651	13.829	14.007	14.185
93	13.580	13.767	13.949	14.131	14.313	14.495	14.677
95	14.242	14.441	14.636	14.830	15.025	15.219	15.414
97	15.278	15.494	15.720	15.941	16.161	16.386	16.603

Table I Continued

P(E,h)	8700	8900	9100	9300	9500	9700	9900	10100
1	8.990	9.059	9.127	9.201	9.274	9.352	9.430	9.508
3	9.063	9.135	9.206	9.283	9.358	9.438	9.519	9.599
5	9.132	9.207	9.281	9.360	9.439	9.522	9.604	9.688
7	9.203	9.280	9.357	9.437	9.518	9.602	9.686	9.769
9	9.276	9.357	9.437	9.521	9.603	9.689	9.775	9.862
11	9.346	9.428	9.511	9.598	9.683	9.772	9.861	9.949
13	9.418	9.503	9.589	9.678	9.766	9.858	9.950	10.041
15	9.489	9.577	9.665	9.757	9.847	9.941	10.035	10.130
17	9.563	9.654	9.745	9.838	9.932	10.028	10.124	10.220
19	9.639	9.732	9.826	9.922	10.017	10.114	10.212	10.311
21	9.706	9.802	9.898	9.998	10.098	10.198	10.299	10.400
23	9.778	9.877	9.976	10.080	10.184	10.288	10.391	10.495
25	9.850	9.951	10.053	10.160	10.267	10.374	10.481	10.588
27	9.921	10.026	10.130	10.241	10.351	10.461	10.571	10.681
29	9.990	10.096	10.210	10.324	10.437	10.551	10.665	10.778
31	10.060	10.169	10.285	10.401	10.517	10.632	10.751	10.870
33	10.133	10.244	10.363	10.481	10.599	10.717	10.838	10.959
35	10.209	10.323	10.444	10.566	10.688	10.809	10.934	11.058
37	10.284	10.401	10.526	10.650	10.775	10.900	11.027	11.153
39	10.361	10.481	10.608	10.735	10.862	10.990	11.119	11.248
41	10.439	10.561	10.691	10.821	10.951	11.081	11.212	11.344
43	10.519	10.644	10.776	10.908	11.041	11.174	11.307	11.441
45	10.599	10.725	10.861	10.997	11.132	11.267	11.403	11.539
47	10.679	10.812	10.950	11.088	11.226	11.363	11.501	11.639
49	10.761	10.901	11.041	11.181	11.321	11.461	11.601	11.741
51	10.849	10.991	11.134	11.276	11.418	11.560	11.702	11.844
53	10.940	11.084	11.228	11.373	11.517	11.662	11.806	11.950
55	11.033	11.179	11.326	11.472	11.619	11.766	11.912	12.059
57	11.132	11.278	11.426	11.575	11.724	11.873	12.022	12.170
59	11.238	11.382	11.528	11.679	11.829	11.979	12.129	12.279
61	11.352	11.495	11.640	11.790	11.940	12.090	12.240	12.391
63	11.469	11.613	11.757	11.908	12.060	12.212	12.363	12.515
65	11.592	11.736	11.880	12.033	12.187	12.340	12.493	12.647
67	11.721	11.866	12.012	12.168	12.324	12.480	12.636	12.792
69	11.859	12.005	12.152	12.311	12.470	12.629	12.788	12.945
71	12.003	12.150	12.297	12.457	12.616	12.776	12.935	13.095
73	12.159	12.308	12.457	12.616	12.775	12.935	13.094	13.253
75	12.324	12.473	12.623	12.785	12.948	13.110	13.273	13.435
77	12.499	12.648	12.798	12.963	13.127	13.292	13.457	13.622
79	12.687	12.839	12.991	13.157	13.323	13.489	13.656	13.822
81	12.897	13.057	13.218	13.378	13.538	13.699	13.859	14.020
83	13.123	13.287	13.450	13.614	13.777	13.941	14.104	14.268
85	13.370	13.538	13.706	13.873	14.041	14.208	14.376	14.544
87	13.645	13.816	13.987	14.158	14.330	14.501	14.672	14.843
89	13.960	14.133	14.306	14.480	14.653	14.826	14.999	15.172
91	14.363	14.541	14.719	14.897	15.079	15.253	15.427	15.601
93	14.859	15.041	15.223	15.405	15.587	15.769	15.956	16.140
95	15.608	15.802	15.997	16.191	16.386	16.580	16.757	16.942
97	16.822	17.050	17.266	17.486	17.703	17.920	18.139	18.355

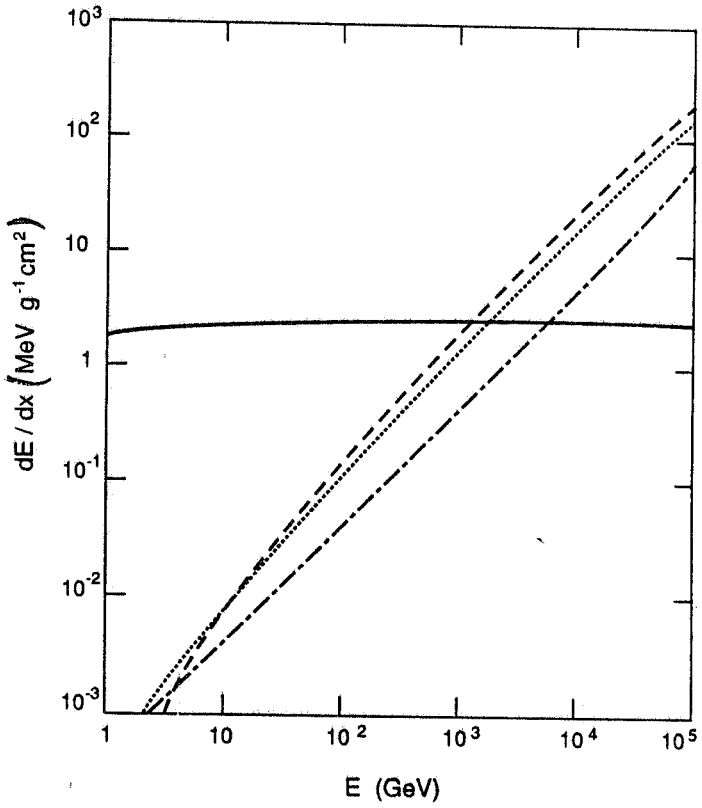

FIG. 1 - Contribution to the muon energy loss in standard rock from ionization (——), pair production (– – –), bremsstrahlung (.....), and nuclear interaction (· – · –) as a function of the energy.

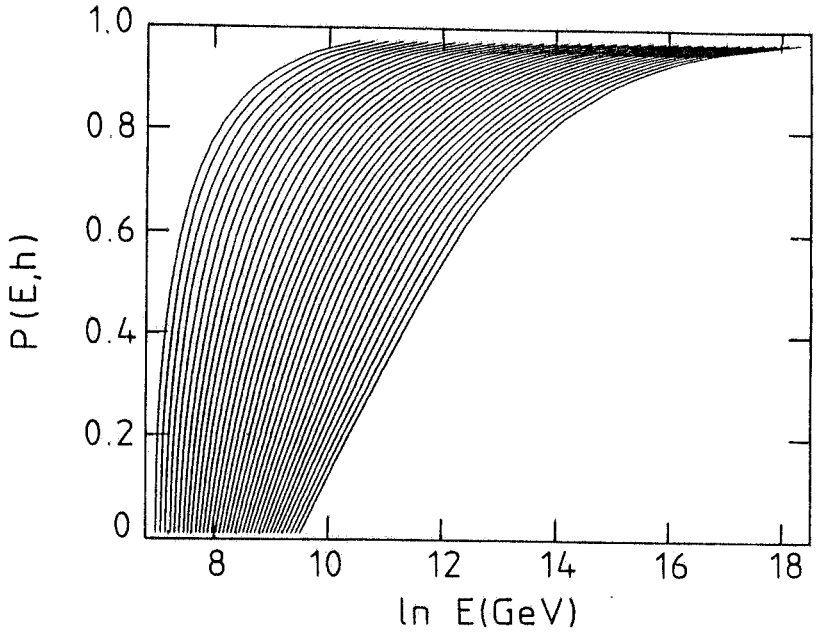

FIG. 2 - Survival probability as a function of the sea-level energy for depths from 3100 to 10100 hg/cm^2 of standard rock in steps of 200 hg/cm^2 (from left to right).

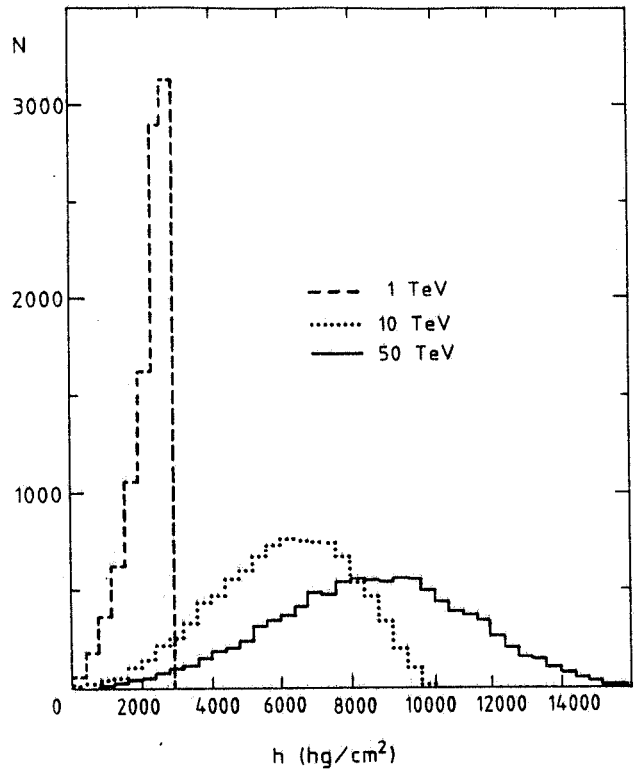

FIG. 3 - The range distribution for muons of energies E = 1, 10, 50 TeV (10^4 entries).

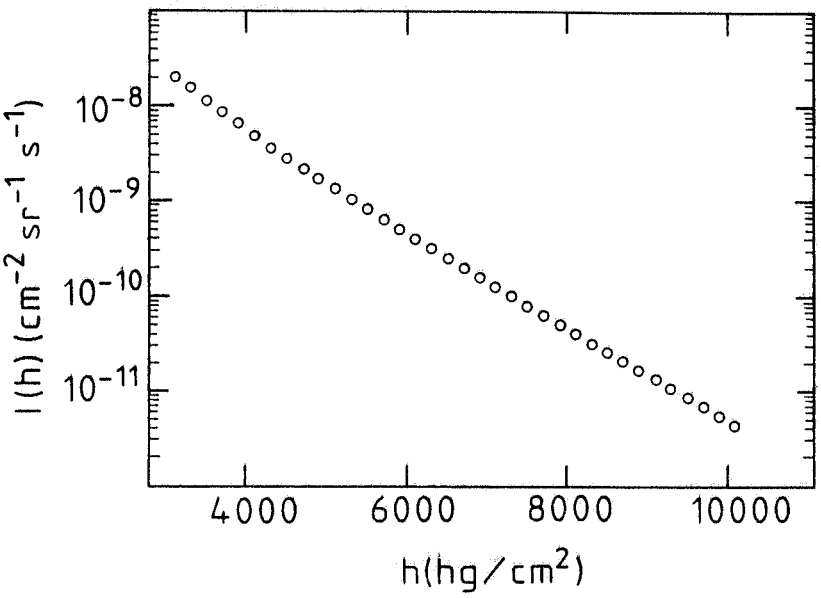

FIG. 4 - The underground intensity I(h) obtained folding the sea-level muon spectrum ~ $E^{-3.71}$ (see text) to the survival probabilities calculated in the present work.

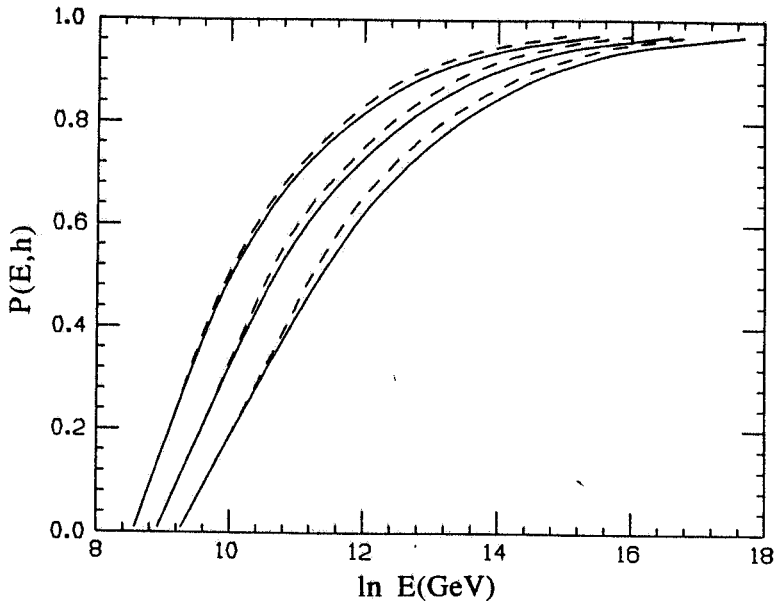

FIG. 5 - Survival probabilities at three depths – 7500, 8500, 9500 hg/cm^2 from left to right side respectively – according to different assumptions on the energy dependence of the photon-nucleon cross section (—— cross section increasing with energy, – – – constant cross section; see text).